Mode-dependent coupling between vibration and translation of product CO_2 in CO oxidation on Pd(111)

Toshiro Yamanaka[a)]
Catalysis Research Center, Hokkaido University, Sapporo 001-0021, Japan

(Received 7 March 2008; accepted 10 April 2008; published online 1 May 2008)

The vibrational temperatures of product CO_2 were measured in CO oxidation on Pd(111) as a function of the desorption angle by means of infrared chemiluminescence. The antisymmetric vibration temperature was separately determined from the other vibrational modes from the normalized chemiluminescence intensity. The product CO_2 desorption is sharply collimated along the surface normal. The antisymmetric vibrational temperature increased from 1300 to 1600 K as the desorption angle increased from 0° to 30°, whereas the averaged vibrational temperature over bending and symmetric modes decreased from 2450 to 1530 K. From these angle dependences, an energy partitioning model in repulsive desorption is proposed. © *2008 American Institute of Physics*. [DOI: 10.1063/1.2918729]

Elucidation of energy transfer dynamics and structures of transition states (TSs) is an important subject for full understanding of surface reaction.[1–11] Such an understanding at the atomic level is required to develop superior catalysts, electrodes, and material growth processes. Dynamics and TS structures can be studied by measurements of translational and internal (rotational and vibrational) energies of desorbing products.[5,12–19] Although angle-resolved (AR) measurements[5–11] are required to study internal energies to obtain detailed structural information, such measurements have long been lacking in thermal surface reactions because of the difficulty of experiments. In this communication, results of measurements of internal energies of AR product CO_2 in CO oxidation on Pd(111) are presented.

CO oxidation on noble metals is a prototypical surface reaction that has long attracted attention of chemists, physicists, and also mathematicians because of its practical importance and rich phenomena.[1,5,11–26] Non-AR measurements of internal energies of product CO_2 have been extensively conducted by analysis of chemiluminescence from CO_2[12–17,19] and infrared (IR) absorption by CO_2.[18] Recently, measurements of internal energies of AR CO_2 have been reported.[27,28] Although CO_2 has three vibrational modes [symmetry stretch (S), bending (B), and antisymmetric stretch (A) modes], in the above AR study, only rotational temperature (T_{rot}) and vibrational temperature (T_{vib}) averaged over the three modes were determined assuming $T_{vib}=T_s=T_b=T_a$ (temperatures of S, B, and A modes).

In this communication, mode-resolved AR measurements of vibrational energies of product CO_2 are presented. The intensity of chemiluminescence from AR product CO_2 was analyzed in comparison with that from high-temperature reference CO_2 from a newly developed molecular beam source, and the degree of excitation of A mode was separately determined from those of other vibrational modes. It was found that the excitations of A and B modes differently correlate with translational directions. In many chemical reactions, it is difficult to experimentally study the moment of reaction, while formation processes of TS structures in surface reactions (including CO oxidation[20–25]) have been studied in detail by *ab initio* calculations. The results of the present study provide unique information on TS structures and subsequent energy partition dynamics.

The design of the apparatus for analysis of extremely weak IR emission from AR CO_2 has recently been described in detail.[27] IR light emitted in relaxation of the antisymmetric stretch mode of CO_2 after passing through two slits for angle selection, $(n_s,n_b,n_a)\rightarrow(n_s,n_b,n_a-1)$, where n_s, n_b, and n_a are the quantum numbers of S, B, and A modes, respectively, is analyzed by a Fourier transform-IR spectrometer. Either a Pd(111) surface or diffusive beam source (1400 K) of reference CO_2 was set before the first slit, and chemiluminescence from product CO_2 and reference CO_2 was detected. The chemiluminescence intensities were normalized by the amount of CO_2 measured by a quadrapole mass spectrometer after the second slit.

The vibrational temperature of A mode was separately determined from the averaged temperature over B and S modes by a careful calibration of chemiluminescence intensity. To compare the intensity from AR product CO_2 with that from reference high-temperature CO_2, a diffusive molecular beam source was newly developed. The reference CO_2 was made to have similar angular distribution and similar temperature to those of product CO_2 on Pd(111), so that all conditions of chemiluminescence measurements are invariant for product and reference CO_2.

The construction of the beam source is shown in Fig. 1(a). After the CO_2 beam passed the two slits, the chemiluminescence from this CO_2 beam was gathered in the same way as that for the product CO_2 in CO oxidation. CO_2 was introduced into a Mo tube heated to 1400 K by a heater made of a Ta wire. The temperature of the Mo tube was monitored with a thermocouple connected at its middle point. This tube was surrounded by Ta double shields and

a)Electronic mail: yama@cat.hokudai.ac.jp.

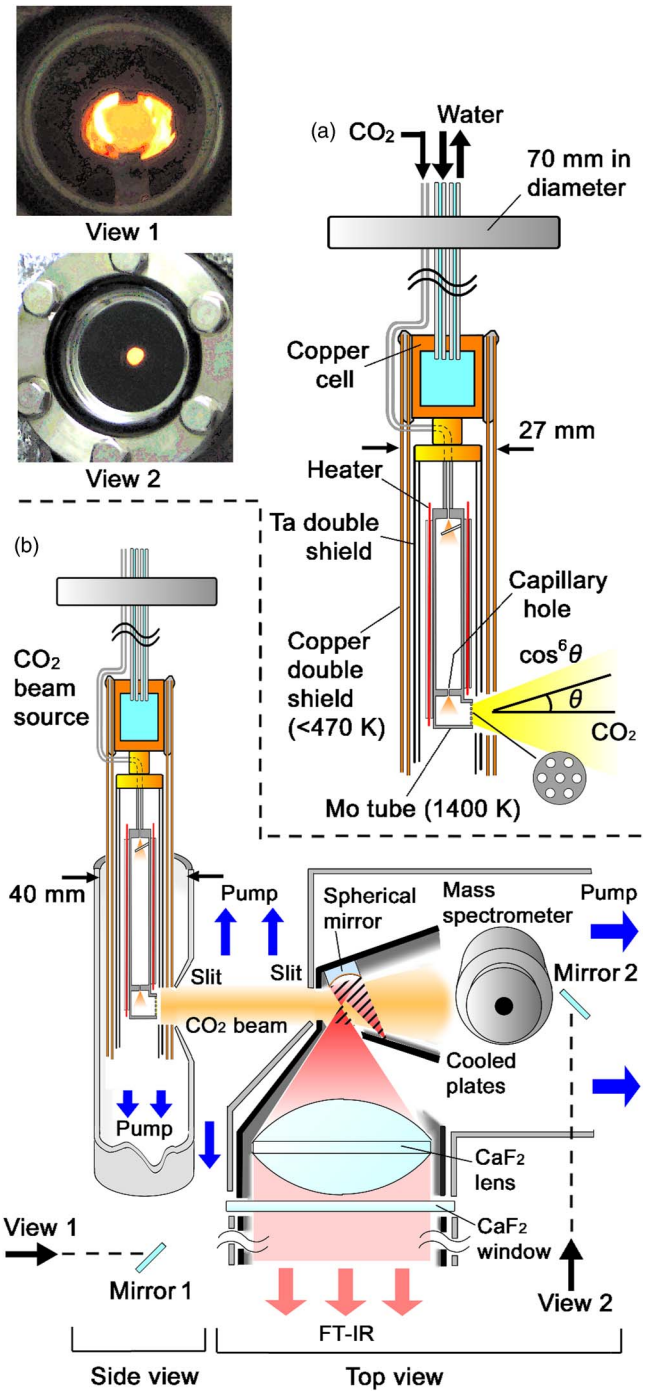

FIG. 1. (Color online) The structure and setup of the molecular beam source.

copper double shields cooled by water, and the surface of the outermost copper shield was kept below 470 K. The diameter of the outermost shield is 27 mm and, thus, this beam source could be set in front of the first slit [Fig. 1(b)], where the distance between the slit and the opposite side of the reaction chamber is only 33 mm. At the upper entrance to the Mo tube, the flow of CO_2 was interrupted by a Mo plate and then CO_2 was emitted through a capillary hole of 0.5 mm in diameter and 4 mm in length. Then, the flow of CO_2 was laterally directed through the final nozzle. This nozzle is a Mo plate of 1 mm in thickness and 10 mm in diameter with seven holes that are each 1 mm in diameter. A theoretical

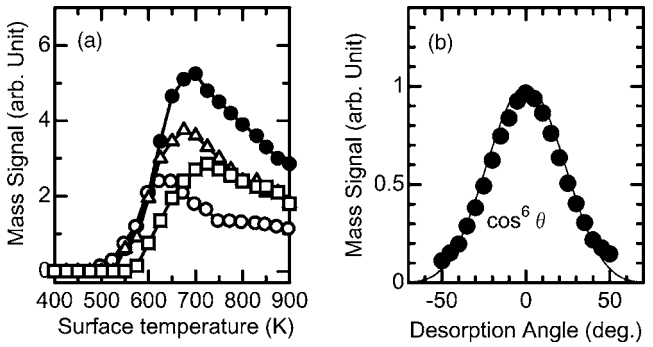

FIG. 2. (a) Rate of CO_2 formation vs T_{surf}. The O_2/CO exposure ratios are 2 (open circles), 1 (open triangles), 1/2 (closed circles), and 1/4 (open squares). The total exposure of CO and O_2 was fixed at 4.5×10^{17} molecules/cm^2 s, and the O_2/CO ratio was varied as indicated. (b) Angular distribution of product CO_2 in the plane along the $[11\bar{2}]$ azimuthal direction. It is sharply collimated along the surface normal.

calculation showed that each hole of which the length and diameter are equal yields an angular distribution of CO_2 close to a $\cos^6\theta$ form.[29] The resultant distribution is close to that of product CO_2 in CO oxidation on a Pd(111) crystal of 10 mm in diameter. The position of the beam source was adjusted by checking images of the beam source reflected by two mirrors set below the beam source in the reaction chamber (view 1) and after two slits in the emission collector chamber (view 2).

Figure 2(a) shows the rate of CO_2 formation versus the surface temperature (T_{surf}) for various O_2/CO exposure ratios at a fixed exposure of 4.5×10^{17} molecules/cm^2 s. At each ratio, with increasing T_{surf}, the CO_2 formation becomes noticeable at above 500 K and shows a maximum at around 650–700 K (T_{max}). Below T_{max}, the oxygen dissociation is rate determining in the CO oxidation, and the surface is highly covered by CO, i.e., $CO(a)\gg O(a)$. The O_2 dissociation increases at higher T_{surf} by increasing vacant sites through enhanced CO desorption. On the other hand, at above T_{max}, the coverage of CO becomes small, resulting in decreasing CO_2 formation. T_{max} shifts to higher values as the O_2/CO ratio decreases because of the higher temperature required to yield vacant sites at high CO pressures.[1,5] The following AR measurements were performed for the optimum CO oxidation at $T_{surf}=700$ K and $O_2/CO=1/2$.

The measurements were limited only in the plane along the $[11\bar{2}]$ direction, since the azimuth effect is negligibly small on a (111) surface.[5] Figure 2(b) shows the angular distribution of product CO_2. The CO_2 desorption was sharply collimated along the surface normal in a $\cos^6\theta$ form, where θ is the desorption angle (polar angle), indicating the repulsive desorption of CO_2 along the surface normal; i.e., nascent CO_2 appears on a repulsive part of potential energy surface.

Each chemiluminescence spectrum (resolution of 4 cm^{-1}) from product CO_2 [Fig. 3(a)] and reference CO_2 [Fig. 3(c)] shows a broad peak consisting of the contributions of transition lines corresponding to a large number of initial rovibrational states. The populations of rovibrational states of product CO_2 are known to be well expressed by the rotational and vibrational temperatures.[12–19] First, the values

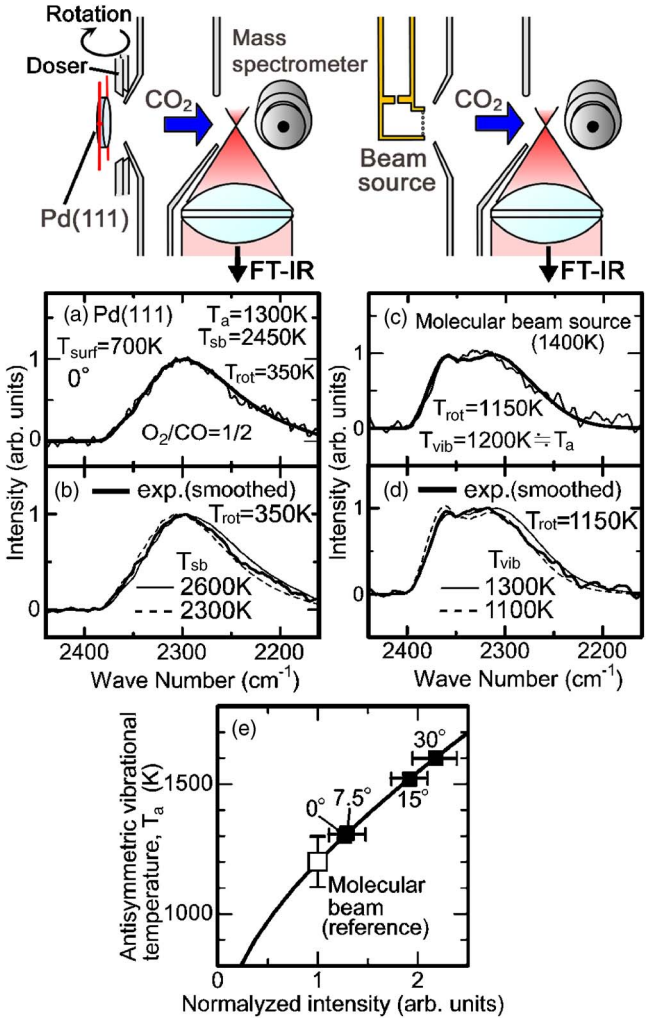

FIG. 3. (Color online) Comparison of chemiluminescence spectra of product CO_2 on Pd(111) at 700 K (The total exposure of O_2 and CO is 4.5×10^{17} molecules/cm^2 s and the ratio of exposure of O_2 to that of CO (O_2/CO) is 1/2.) and reference CO_2. In (a) (product) and (c) (reference), thin lines and thick curves show experimental and optimum simulated results, respectively. (b) and (d) show smoothed experimental results (thick solid curves) and some simulated curves (thin solid and thin dashed curves), indicating that error bars of T_{sb} and T_{vib} are close to 150 and 100 K. (e) Determination of T_a by plotting chemiluminescence intensity normalized by CO_2 mass signals. The curve indicates theoretical calculation (see text).

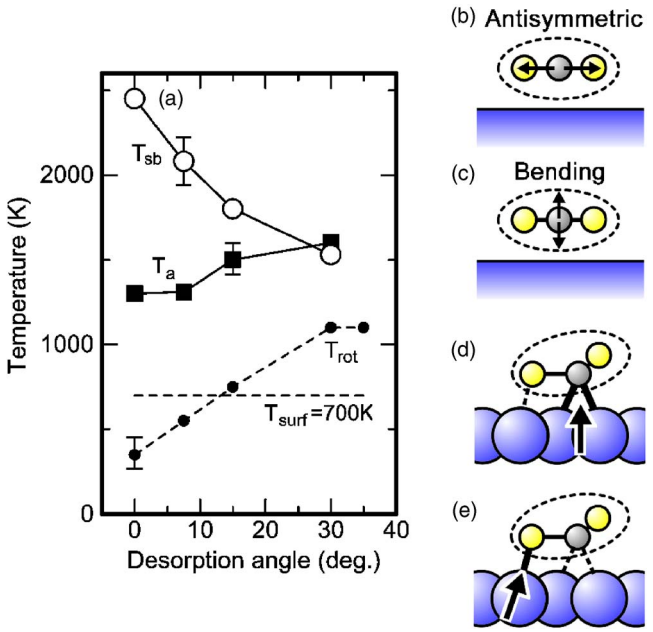

FIG. 4. (Color online) (a) Angular dependence of T_a, T_{sb}, and T_{rot}. The error bars in (a) were estimated without considering the uncertainty of T_a (100 K) of the reference CO_2. An increase in T_a of reference CO_2 by 100 K leads to increases in T_a by about 100 K and decreases in T_{sb} by about 30 K at all desorption angles. (b)–(e) show illustrations of TSs with directions of vibration and repulsion.

of T_{rot} and T_{vib} of the reference CO_2 were determined by curve fitting of the experimentally obtained spectrum with simulated ones.[12,27,30] The spectrum is wide when T_{rot} is high, while the spectrum is more redshifted when each of T_s, T_b, and T_a is high. In the simulation, the ratio of redshift with increases in T_s, T_b, and T_a was about 1:2:1.3. Since T_s, T_b, and T_a could not be separately estimated only from the degree of redshift, T_{vib} averaged over the three modes (i.e., assuming $T_{vib}=T_a=T_s=T_b$) and T_{rot} were estimated. The experimental spectrum lies at a lower (higher) wavelength than the simulation for $T_{vib}=1100$ (1300) K [Fig. 3(d)], showing the error bar close to 100 K. The thick curve in Fig. 3(c) shows the optimum simulated result yielding $T_{vib}=1200$ K and $T_{rot}=1150$ K. These values are lower than the temperature at the center of the beam source (1400 K), probably because the temperature around the final nozzle is lower. Since these values are close to each other, the internal modes are almost in equilibrium, i.e., $T_a\approx1200$ K. The total chemiluminescence intensity changes with T_a in the following form as shown by the solid curve in Fig. 3(e):

$$I_{tot}=\sum_{na=1}^{\infty}R_V^{\,2}\exp(-E_{na}/kT_a)/\sum_{na=0}^{\infty}\exp(-E_{na}/kT_a),$$

where $R_v^{\,2}$ is Frank–Condon factors and E_{na} is the energy of antisymmetric vibration. Thus, T_a of product CO_2 was obtained by comparing total intensities of the chemiluminescence normalized to the CO_2 mass signals from product CO_2 and that from reference CO_2 in Fig. 3(e). In Fig. 3(e), the theoretical curve is normalized so that I_{tot} at $T_a=1200$ K (T_a of reference CO_2) becomes unity. The obtained values for T_a are 1300, 1310, 1500, and 1600 K at $\theta=0°$, 7.5°, 15°, and 30°, respectively. Then, the temperature of the other two vibrational modes (T_{sb}) of product CO_2 was determined by curve fitting assuming $T_{sb}=T_s=T_b$, since T_s and T_b could not be separately estimated only from the degree of redshift. The contribution of the B mode to T_{sb} is twice that of the S mode, since CO_2 has two kinds of B modes of which vibrational directions are perpendicular to each other. The thick curve in Fig. 3(a) shows the optimum result yielding $T_a=1300$ K [obtained by Fig. 3(e)], $T_{sb}=2450$ K, and $T_{rot}=350$ K. A similar estimation of T_a in CO oxidation has previously been reported.[29] The values of T_a, T_{sb}, and T_{rot} are summarized as functions of desorption angle in Fig. 4(a). T_{sb} decreases while T_a and T_{rot} increase as the desorption angle increases.

The different angular dependence between T_a and T_{sb} indicates that A and B modes differently couple to the translational mode in their excitation processes. When TS leaves the surface to become CO_2, the excess energy is partitioned into translational, vibrational, and rotational modes. The bent

TS (Refs. 20–22) becomes linear and the C–O bond lengths approach that of gas-phase CO_2, resulting in vibrational motions. These structural changes from TS to linear CO_2 may induce an impulse accelerating the translational motion in the same direction as that of vibration; i.e., vibrational and translational motions in the same direction are thought to be strongly coupled to each other. If TS is parallel to the surface, the directions of vibrational motions of *A* and *B* modes are parallel and perpendicular to the surface, respectively [Figs. 4(b) and 4(c)] and, thus, desorption of CO_2 with highly excited *A* and *B* modes is promoted in parallel (inclined) and perpendicular directions, respectively.

A more detailed picture is considered as follows. It is natural to expect that CO approaches O to form an upright TS, since diffusion of CO is much faster than that of O at 700 K. However, theoretical modeling indicates that, even though free diffusion of the O atom does not occur, a TS is formed by motion of both CO (diffusion) and the O atom (movement from threefold to twofold Pd bonding); the transition state has both the C end of CO and the O atom bonded to the same Pd atom. The TS is nearly surface parallel and bent,[21–23] as illustrated in Fig. 4(d), leading to the final state in which the CO_2 molecule is horizontally lying.

In the TS, three bonds of Pd–O, Pd–CO, and O–CO compete with each other. When the Pd–CO bond is strong and the Pd–O bond is weak, TS may become more bent and more symmetric with respect to the C atom and the surface normal direction. Nascent CO_2 receives repulsion in the symmetric (surface normal) direction at the C end close to the center of mass, resulting in the normally directed desorption of CO_2 with high T_{sb}, low T_a, and low T_{rot}. In contrast, when the Pd–O bond is strong and the Pd–CO bond is weak [Fig. 4(e)], TS may become more linear and more antisymmetric with respect to the C atom and the surface normal direction. Nascent CO_2 receives repulsion in the antisymmetric (inclined) direction at the O end far from the off center of mass, resulting in inclined desorption of CO_2 with high T_a, high T_{rot}, and low T_{sb}.

In the present work, T_{sb} was higher than T_a, while in the previous work, T_a was higher than T_s and T_b on Pt polycrystalline. Probably to keep Pd–O, Pd–CO, and O–CO bonds, TS must be bent on flat Pd(111) [Fig. 4(d)], resulting in high T_{sb}, while TS can be linear at corrugated step or kink sites on polycrystalline.

The present work showed that the angular dependence of vibrational excitation is mode dependent, which provides valuable information on TS and dynamics. Together with advanced theoretical works, AR measurements of internal energy will unveil new microscopic features in surface chemical physics.

I thank Professor Tatsuo Matsushima for supporting this work. I thank Professor Kiyotaka Asakura for stimulating discussion. This work was partially supported by Grant-in-Aid No. 17350002 for General Scientific Research from the Japan Society for the Promotion of Science.

[1] R. Imbihl and G. Ertl, Chem. Rev. (Washington, D.C.) **95**, 697 (1995).
[2] F. M. Zimmermann and W. Ho, Surf. Sci. Rep. **22**, 127 (1995).
[3] A. Hodgson, Prog. Surf. Sci. **63**, 1 (2000).
[4] H. A. Michelsen, C. T. Rettner, and D. J. Auerbach, Phys. Rev. Lett. **69**, 2678 (1992).
[5] T. Matsushima, Surf. Sci. Rep. **52**, 1 (2003).
[6] R. T. Jongma, G. Berden, T. Rasing, H. Zacharias, and G. Meijer, J. Chem. Phys. **107**, 252 (1997).
[7] H. Vach, A. De Martino, M. Benslimane, M. Chatelet, and F. Pradere, J. Chem. Phys. **100**, 8526 (1994).
[8] F. H. Geuzebroek, A. E. Wiskerke, M. G. Tenner, A. W. Kleyn, S. Stolte, and A. Namiki, J. Phys. Chem. **95**, 8409 (1991).
[9] J. W. Elam and D. H. Levy, J. Chem. Phys. **106**, 10368 (1997).
[10] S. L. Bernasek, M. Zappone, and P. Jiang, Surf. Sci. **272**, 53 (1992).
[11] C. T. Campbell, G. Ertl, H. Kuipers, and J. Segner, J. Chem. Phys. **73**, 5862 (1980).
[12] D. A. Mantell, K. Kunimori, S. B. Ryali, G. L. Haller, and J. B. Fenn, Surf. Sci. **172**, 281 (1986).
[13] S. L. Bernasek and S. R. Leone, Chem. Phys. Lett. **84**, 401 (1981).
[14] L. S. Brown and S. L. Bernasek, J. Chem. Phys. **82**, 2110 (1985).
[15] G. W. Coulston and G. L. Haller, J. Chem. Phys. **95**, 6932 (1991).
[16] C. Wei and G. L. Haller, J. Chem. Phys. **103**, 6806 (1995).
[17] C. Wei and G. L. Haller, J. Chem. Phys. **105**, 810 (1996).
[18] D. J. Bald, R. Kunkel, and S. L. Bernasek, J. Chem. Phys. **104**, 7719 (1996).
[19] H. Uetsuka, K. Watanabe, H. Ohnuma, and K. Kunimori, Chem. Lett. **25**, 227 (1996).
[20] A. Alavi, P. Hu, T. Deutsch, P. L. Silvestrelli, and J. Hutter, Phys. Rev. Lett. **80**, 3650 (1998).
[21] C. J. Zhang and P. Hu, J. Am. Chem. Soc. **123**, 1166 (2001).
[22] P. Salo, K. Honkala, M. Alatalo, and K. Laasonen, Surf. Sci. **516**, 247 (2002).
[23] See: http://www.fyslab.hut.fi/~pts/CO_oxidation.html
[24] J. Rogal, K. Reuter, and M. Scheffler, Phys. Rev. Lett. **98**, 046101 (2007).
[25] X.-Q. Gong, Z.-P. Liu, R. Raval, and P. Hu, J. Am. Chem. Soc. **126**, 8 (2004).
[26] V. P. Zhdanov, Surf. Sci. Rep. **45**, 233 (2002).
[27] T. Yamanaka and T. Matsushima, Rev. Sci. Instrum. **78**, 034105 (2007).
[28] T. Yamanaka and T. Matsushima, Phys. Rev. Lett. **100**, 026104 (2008).
[29] B. B. Dayton, *Proceedings of the National Symposium on Vacuum: Technology Transactions* (Pergamon, London, 1957) p. 5.
[30] K. Nakao, S. Ito, K. Tomishige, and K. Kunimori, J. Phys. Chem. B **109**, 17553 (2005).